# Changes of the Electrical and Optical Character of Polyimide Films (and the Chemistry that Drives Them) Due to Exposure to High Energy GEO-like Electrons

**Ryan Hoffmann**
*AFRL/RV*
**Russell Cooper**
*Assurance Technology Corporation*
**David Wellems**
*Applied Technology Associates*
**Dale Ferguson**
*AFRL/RV*

**AMOS 2015 CONFRENCE PAPER**

## 1. ABSTRACT

As a result of the interaction between the spacecraft and its operational environment, the constituent materials begin to change. These changes are determined by a combination of energy deposition, the resulting chemical reactions, and contamination. These changes negatively impact the ability of spacecraft operators to predict the behavior of a spacecraft as it ages. For example, in the case of electrical conduction in polyimide, there is a three orders of magnitude decrease in the resistivity after only eight months of simulated GEO electron exposure. This will affect the results of models designed to predict the spacecraft electric potential a spacecraft will adopt and could lead operators to fly a spacecraft in unsafe conditions. Optical changes in the material also dramatically impact the ability of ground based optical observations to identify and track both known and unknown spacecraft.

We are presenting work to quantify the changes in total reflection and electrical conduction of aluminized polyimide film after simulated aging in a GEO-like electron environment. We correlate these data with the chemical structure of the film as determined by X-Ray Photoelectron Spectrometry (XPS). A deeper, predictive understanding of how materials change will not only increase the operational lifetime of space assets by improving material selection, it will also improve space situational awareness (SSA) by allowing ground based observers to more accurately deduce component materials and determine how long a spacecraft has been in orbit.

## 2. INTRODUCTION

Spacecraft are made of a variety of materials, many of which are disordered dielectric materials such as polyimide (PI). [1] The US Air Force is interested in material properties for a variety of reasons, two of which we focus on in this paper: understanding susceptibility of spacecraft to space weather, and optical characterization of satellites for SSA. This study focuses on polyimide, a common space material which has a rich history in both ground based and space experiments. These experiments have shown both electrical and optical changes in PI due to exposure to the GEO space environment. Ground-based experiments have shown electrical conductivity increases after exposure to each individual component of the space environment: electrons[2, 3], photons[4], and ion bombardment. [5-7] Although these limited ground based studies have shown optical and electrical changes to PI, the chemistry and physics underlying these changes is not yet well understood. The chemistry of PI has been addressed in a small body of literature, but the interpretation of these studies have not focused on charge transport or optical changes.[8] Most of the previous studies of PI related to charge transport have focused on pristine materials.[9-11] While they have learned much about the role of radiation induced conductivity, photoconductivity, temperature, etc., the ability of the spacecraft operator to use this information is limited by the fact that materials in space are no longer pristine.

This paper shows that PI undergoes dramatic changes in its electrical resistivity when bombarded by high energy electrons. These changes are correlated with gas evolving from the surface. Surprisingly, despite the dramatic electrical and chemical changes of the PI, the optical properties of PI undergo minimal changes.

## 3. EXPERIMENT

The work included in this publication was completed in the Spacecraft Charging and Instruments Calibration Lab (SCICL) located on Kirtland Air Force Base. This laboratory is part of the Space Systems Survivability program of the Space Vehicles Directorate (RV).[12] This work was accomplished in the Jumbo Environmental Simulation Chamber which can simulate a large fraction of the charged particle environment for both the GEO and LEO. For a full description of the Jumbo chamber capabilities please refer to the AF technical.[13]

In order to examine the electrical and optical properties of aged material it was necessary to divide the experiment into four phases; aging, electrical testing, optical testing, and chemical analysis. Before testing each material was cleaned using isopropyl alcohol. The samples were attached to the aluminum disk (sample carousel) by use of double sticky Cu tape with conductive adhesive affixed to the Al coated side of the sample. The use of the Cu tape provides both the mounting mechanism and the ground plane for the material. The sample carousel was placed in a vacuum oven pumped to <100 mTorr and heated to 60° C for 48 hr in order to drive off contamination such as water. Studies at room temperature show that water is the main contaminant (>99%) and that exposure to vacuum decreases the outgassing rate four orders of magnitude in ~12 hr.[14] It is reasonable to assume that the elevated temperature accelerates this rate and that most of the water is driven from the surface after the bake out is complete. The sample carousel is then removed and quickly (<20min) mounted in the Jumbo chamber and pumped to $10^{-7}$ torr overnight.

Materials are aged by bombardment with fully penetrating radiation in order to expose them to an approximately uniform dose through the bulk of the material. We use 25 μm and 50 μm films and 90 keV electrons which fully penetrate the thin films for uniform aging.[15] These films are manufactured by Sheldahl and have part numbers 146446 and 146448 respectively.[16] To create uniform exposure, the samples rotate continuously on the carousel with the axis of rotation parallel to the electron beam. Surface potential is measured with a high voltage Trek 341B non-contact surface volt meter. Measuring near zero surface potential during aging verifies that the electrons are fully penetrating, however, a small residual surface charge of ~100V is induced, presumably due to secondary electron emission from nearby surfaces.[2, 17] The electron dose delivered to a material is given by

$$dose\ rate = \frac{JE}{\rho q_e R} \qquad \text{(Eq. 1)}$$

where $J$ is the electron flux, $E$ is the electron energy, $\rho$ is the material density ($1.4 \times 10^{-3}$ kg/cm$^3$ in the case of PI), $q_e$ is the charge on an electron and $R$ is the electron penetration range as calculated by the NIST ESTAR database. [15] To make the correlation to the electron dose in GEO we use the AE9 model and determine the differential flux of electrons. [18] It is now simply a matter of integrating all energies (from 40 keV to 7 MeV available in the model) to arrive at a total dose rate of 0.215 Gy/s delivered by electrons to PI< 50 μm thick on orbit. The PI in this study has undergone aging from 0-$5 \times 10^6$ grey, which corresponds to 0-8months in GEO. During aging, we monitor the flux of the electron gun with a Faraday cup mounted beside the sample carousel. The spatial distribution of electrons has been thoroughly mapped, allowing calculation of the electron flux over all samples by measuring current on the Faraday cup. The Faraday cup also allows for on-the-fly correction of the ~1% hr drift in electron beam flux, thus allowing for accuracy in achieving our target dose.

The electrical characterization is accomplished in Jumbo and generally started the day after the aging is complete, without breaking vacuum. We measure charge transport by monitoring the surface potential of the thin films during bombardment with low flux, ~30pA/cm$^2$, 20keV electrons. This is done using a ±20 kV non-contract electrostatic voltmeter manufactured by Trek™. These electrons do not fully penetrate the material and therefore charge the material to a negative potential. The relatively low flux and energy of the charging beam delivers ~600 Gy to the material and the electrons penetrate to a depth of R=7 μm. Not only is this dose negligible, relative to the aging dose, it only effects the area between the top surface and the penetration depth. Since the grounded plate is on the rear surface, the electrons will migrate in that direction and therefore will not interact with the top region. We monitor the materials charging until the surface potential reaches a quasi-equilibrium state. The electron gun is then switched off and the surface potential is monitored as a function of time as the deposited electrons drift toward the grounded back plane. It can take days until the potential on the samples approaches 0 V. We use previously developed models to fit this data and derive the bulk conductivity. [9-11, 19]

After aging and measuring discharge rates we remove small pieces of each material for use in XPS chemical analysis. The remaining sample is then used for optical analysis. XPS was carried out at the Center for Micro-Engineered Materials (CMEM) at the University of New Mexico. We used a Kratos AXIS ULTRA XPS to measure accurate elemental composition of the surface and, more importantly, quantitatively identify the chemical environment and electronic states of the elements. To characterize the optical changes after aging we chose to use directional-hemispherical reflectance (DHR) as a first pass at understanding the optical changes. This was done using both Perkins-Elmer λ-950 and a SOC 400T spectrometer with a combined spectral range of 0.2-25 µm.

## 4. Results

### 4.1 Electrical Behavior

As mentioned above we monitor the surface potential of PI as it is charged by exposure to a 20keV beam of electrons. As the sample is exposed, some electrons are captured and a negative surface potential develops. Once an equilibrium potential is reached the beam is extinguished and the imbedded electrons begin to migrate to the grounded back pane. This migration causes the surface potential to decay giving us a measure of surface potential as a function of time.

The first part of the decay is driven by the electrons transporting toward the grounded plane, but have yet to reach the back plane and exit the material. This portion of the curve is termed the pre-transit decay and can be related to the intrinsic mobility of electrons hopping from one trap state to the next. [9] Characterization of the pre-transit decay is beyond the scope of this paper, however it is critical to determine when the charge body reaches the back plane so that the dark conductivity can be determined. This is done by noting when the decay curve transitions to a straight line when plotted on a log-log scale. This time is termed the transit time $t_T$ and marks the beginning of the power law behavior that is driven by the dark conductivity.

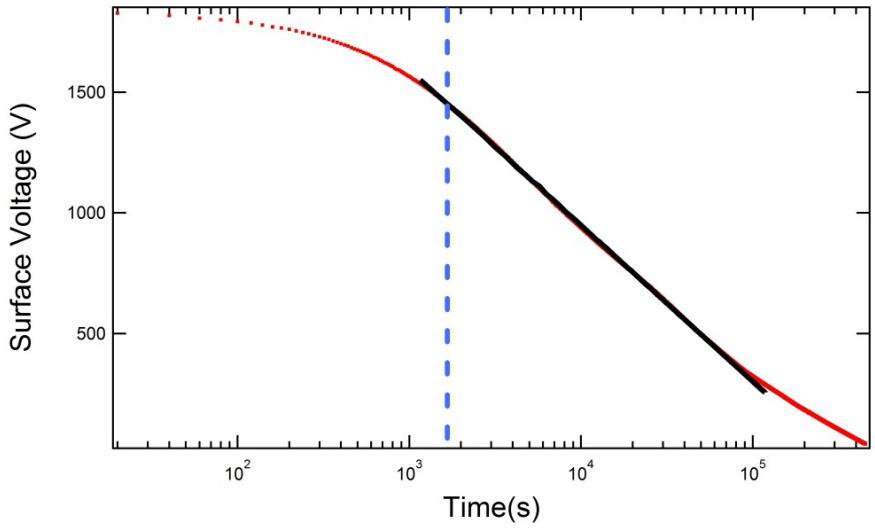


*Fig. 1 The surface potential decay of un-aged PI that was charged with a 20 keV electron beam. The black line is then fit to Eq. 1 with a $\tau_{decay}$ of 12 hr from which we derive a dark conductivity of 1.5e-15 Ωm. We determined the transit time $t_T$ to be 28 min.*

After the front of the charge body has reached the grounded backplane, the dissipation of charge is primarily determined by the loss of electrons from the material. This region is fit by Eq. 2 from which we are able to derive a decay time and the dark resistivity of the material. [10]

$$V_s\left(\tau_{decay}\right) = m{\tau_{decay}}^{b} \qquad \text{(Eq. 2)}$$

$$\rho_{dark} = \frac{\tau_{decay}}{\epsilon_0 \epsilon_r}$$

Dark resistivity $\rho_{dark}$ is critical because it is the macroscopic behavior that characterizes charge transport on long time scales and is often the only parameter reported in the literature. Dark resistivity is the true measure of the ability for a material to transport charge and is non-varying as a function of time like the pre-transit decay. It also allows for comparisons between this and work on resistivity undertaken with alternative experimental studies that might not have the other parameters we use in this study. We calculate the bulk resistivity of pristine PI to be ~$2x10^{15}$ Ωm and that is in good agreement with the value of $1.8x10^{15}$ Ωm published by the manufacturer. [16]

Five sets of PI were exposed to different amounts of electron radiation. Each set consists of 25 µm and 50 µm Al backed and 25 µm Cu tape backed PI films. The first set is the pristine material that underwent all the same environmental conditions as the others, however was not exposed to aging electrons. The remaining sets were exposed to 6.7 $x10^5$ Gy, 2.0 $x10^6$ Gy, 3.9 $x10^6$ Gy, and 4.5 $x10^6$ Gy corresponding to 1.2, 3.5, 6.8 and 7.9 months of GEO electron radiation respectively. There is a marked decrease in the resistivity between the pristine and least aged sample, 6.7 $x10^5$ Gy, and then the resistivity appears to level off with aging, as can be seen in Fig. 2. This is most likely due to the limitation of our method of determining resistivity and not a real plateau. Because our method required that the material store charge for tens of minutes in order to determine decay rates, the decay time cannot be less than this. In fact the final data set that was exposed to 4.5 $x10^6$ Gy (7.9 months GEO electron dose) did not charge at all and could not be included in Fig 2. It is likely that the material continues to exhibit enhanced conductivity as the dose increases, but would require other methods to measure. This does provide an upper bound for conductivity. However, if we look at the equilibrium voltage that each sample reached before the beam was extinguished as shown in the righ plot of Fig.2, we see a continual reduction as the materials age. Since the changing beam varied less than 40%, in flux, the reduction in peak voltage can only be due to the fact that the material is better at transporting charge through the bulk and into the grounded back plane.

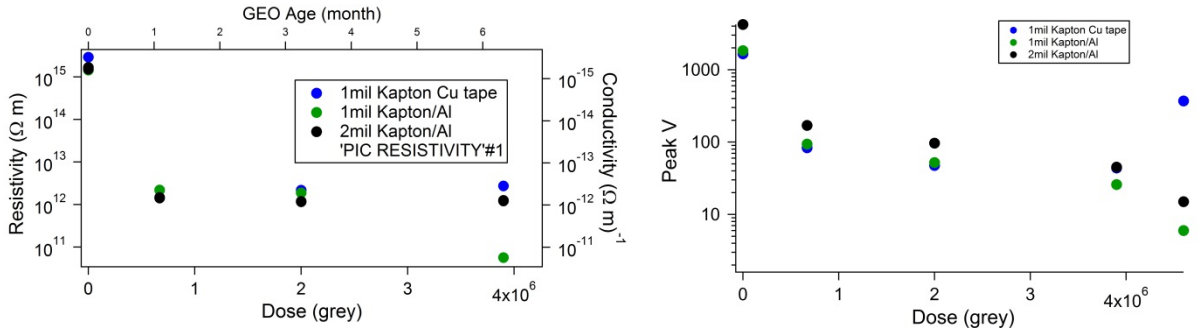


*Fig. 2. (Left) Resistivity of 25 µm PI with Cu tape backing, Al backing and 50 µm PI with Al backing shown as a function of aging dose. (Right) Quasi-equilibrium potential reached immediately after the charging beam was extinguished.*

### 4.2 Optical Behavior

After the electrical tests, the materials were removed from the vacuum chamber and directional hemispherical reflectance (DHR) was performed in air. This test took place several months after the initial aging. The samples were kept clean, however it is assumed that all the chemistry induced by aging has taken place. The DHR of the 25 µm material (top row of Fig. 3) does show what might be a slight increase in reflectivity of 1.5% on the right side of the band edge of ~2.3 eV. This trend does not continue in to the IR so it is difficult to say if it aging related or an experimental artifact. Assuming that the 1.5% shift is real it is interesting to note that the reflectance near the band edge seem to follow the same trend as the conductivity measurements, i.e. that most the change is seen between pristine and the first dosing.

For wavelengths larger than the 2.3 eV bandgap, we expect the DHR of the 50 um PI sample to be less than the 25 um sample because there is more attenuation along the longer primary optical path. The front surface of PI is only a few percent reflective across the 2-25um wavelength range and the majority of the reflection occurs at the aluminum back surface. For the 2- 25 um wavelength range and with the thicker sample, the DHR is necessarily smaller. For the thicker sample, the aging impact on attenuation is apparent in that the path loss is reduced, or the DHR increased.

For wavelengths smaller than the bandgap, the 25 um sample DHR is somewhat higher than the 50 um sample because of back plane reflection. Surface reflection is the dominant contribution to the DHR for the thicker sample. In general, with increasing PI thickness, the transmission lines broaden and weaken and the sharpness of 2.3 eV PI bandedge is reduced.

In the 50 µm material there is no discernable trend in the short wavelength DHR except that the 2.0x $10^6$ Gy material was much less reflective, we attribute this to a mounting differences between it and the other samples. There is a trend in the mid-IR DHR toward becoming more reflective as the materials age and, most of the change appears to happen between the pristine material and the first dosing. In fact, the mid-IR band reflectance increases 34% with most of that changes happening at <6.7x$10^5$ Gy. PI has an extremely complicated absorption spectrum in the mid-IR, however on close examination of the some of the trends insights in to aging chemistry are reviled. The absorption line at 12 µm shows a clear upward trend with dose and can be correlated to a loss of C-N bonds. [8]

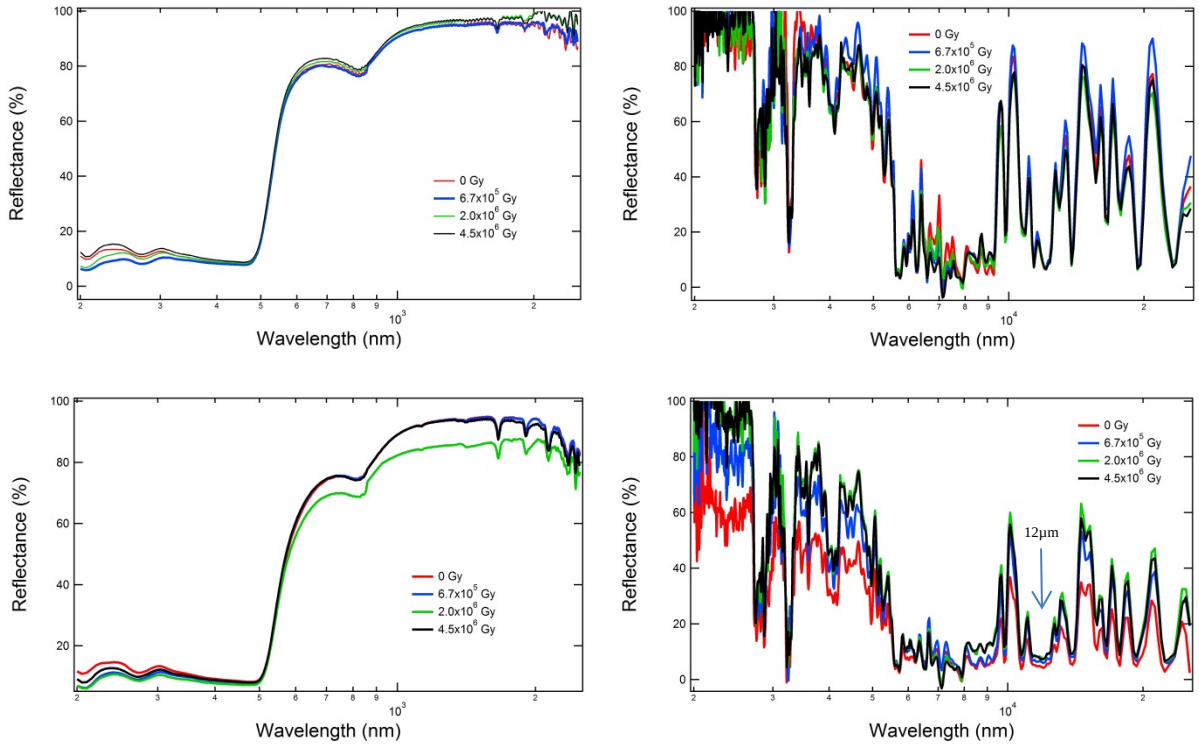


*Fig. 3 DHR measurements of 25 µm (top row) and 50 µm (bottom row) of Al backed PI. Each trace is the reflectance of the samples as a function of the electron dose they were exposed to.*

Birefringent studies may reveal more subtle optical changes taking place in PI as it ages. They might take the form of a reduction in the bidirectional reflectance distribution function (BRDF) ps/pp ratio or, for PI, a migration in the optical axis. A study of these properties was initiated, but such measurements are highly dependent on surface roughness, sample mounting, and tensioning. As such, it was impossible to directly compare one sample to the next, however, we can say that all the samples remained birefringent.

### 4.3 Chemical Analysis

We are able to use XPS tests to help elucidate the chemistry occurring in PI during electron radiation. XPS is only sensitive to the first few layers of the material, however due to the nature of the electron energy loss mechanism, it is likely that the surface chemistry closely mimics that of the bulk. XPS yields elemental composition of the sample as well as bonding information on the individual components. The two most striking XPS results are shown in Fig. 4. The XPS shows a decrease in the elemental fraction of oxygen between pristine samples and those with a 5x$10^5$ Gy, which then increases with further aging. The measured oxygen is below the percent as dictated by the monomer unit.

This could be due to molecular orientation on the surface. It is possible, although unlikely, that this is due to material contamination. Similar elemental composition on pristine samples using XPS has been previously seen with oxygen representing 15.1% of the composition.[20] The fraction of carbon that is bound to a nitrogen or oxygen atom also undergoes an initial drop followed by a recover to near the pristine state. We noted a dramatic increase in chamber pressure during aging and we attribute to outgassing of species that have been created by bond breaking in the PI. As time progresses the chamber pressure drops, indicating decreased outgassing, however it does not return to its baseline. This indicates that gas evolution from PI plays an important role in the chemistry of PI. To understand the change in elemental composition we draw on two different studies of irradiation PI and evolution of gaseous species from these samples. These studies were undertaken with very different

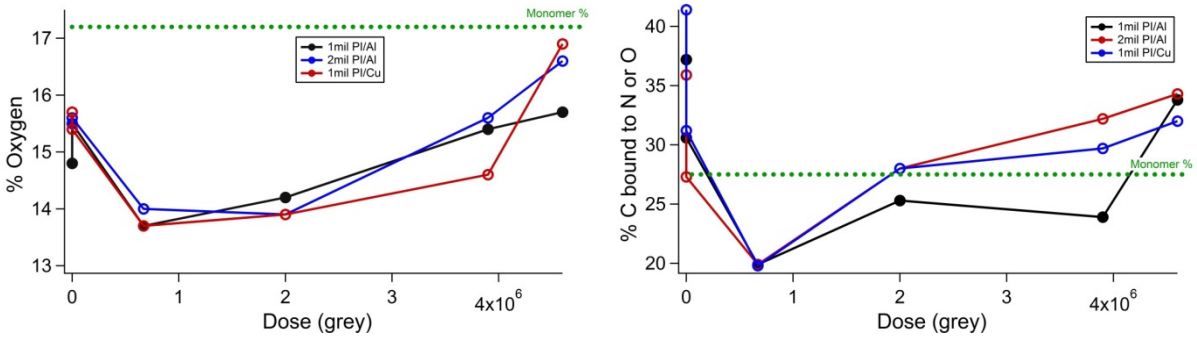


*Fig. 4 XPS results on PI as a function of dose. The upper plot shows the elemental fraction of oxygen in the PI for three different samples 1mil PI backed by Al, black, 2 mil PI backed by Al, red, and 1mil PI backed with Cu tape, blue. The theoretical fraction is shown as a dashed green line. The lower plot shows the fraction of carbon that is electron poor for the same three PI samples.*

conditions, both from each other, and from our set-up, but the chemistry they propose is consistent with the measurements here. These studies were undertaken with different energetic particles and cover a wide energy range energy, but the chemistry they propose is consistent with the measurements here. Oxygen is lost as CO, $CO_2$, and $H_2$, is evolved from the material.[8] Our XPS results indicate the oxygen that has double or triple bonds is preferentially lost to oxygen that does not, which is in line with our theory and the results seen in the mid-IR DHR results in the 50 µm material. Decreases in oxygen to 12% have been previously seen in proton bombardment, although we don't see this extent of change our results agree qualitatively.[20] Other PI degradation experiments found that with 760MeV Kr ion bombardment that the major gas species evolved from the system were mainly hydro- deficient chain fragments of the form of CxH2x-y (x varies from 1 to 6, for each x, there are several y).[21] It is likely that both of these mechanisms play a role in the degradation chemistry, but that the relative importance of each varies with dose.

## 5. CONCLUSION

This study has leaned heavily on previous work involving ion bombardment of PI and the chemical changes caused by the ion radiation damage. However, there is one striking difference between our work and those that bombard with ions, and that is the lack of optical changes of the PI in our work. Other work has generalized the change in optical properties as occurring at lower doses then the change in electrical, although this might be more material specific than the authors originally thought.[22] With extensive ion bombardment the PI becomes quasi-conductive, mechanically brittle, and black. From this work a 14 eV/nm$^3$ energy threshold for damage of PI was found by ion bombardment and used as justification for the dramatic changes in electrical conductivity.[7] Although changes in PI resistivity presented here are not of the magnitude presented in ion bombardment, it is possible that electron bombardment has a more dramatic impact on the electrical properties of the material than optical or mechanical. This is a somewhat surprising result as radiation dose is often thought to be independent of the particle doing the radiation. [23] However, as seen here, this is not always the case.[24, 25]

We have presented the resistivity of PI samples that have been irradiated by penetrating electrons. The resistivity undergoes a dramatic change, three orders of magnitude, at 5x10$^5$ grey and likely continues to decrease at doses above that to 5x10$^6$ grey, although the lower limit of our current experimental techniques has been reached. DHR

measurements show a trend toward increased reflectivity in the mid-IR with most of that change happening at the same dose as the dramatic change as the resistivity. XPS measurements of surface chemistry show initial decrease in oxygen presence due to radiation, which then further increase with time. We see gas evolving from the surface during irradiation and hypothesized that gas is predominately CO, $CO_2$, and $H_2$ at early times and unsaturated alkanes at later times, as has been seen for ion irradiation and this mechanism is supported by the XPS and DHR results. Compared to PI degradation due to heavy ion bombardment, we saw a comparably smaller change in PI's properties, although the difference in the change does not seem to be consistent across all properties. It is unclear for PI if the chemical reactions caused by radiation damage are merely slower for electron radiation than ion bombardment, or if it is fundamentally different chemistry.

## 6. ACKNOWLEDGMENTS

We recognize support from AFOSR Materials for Extreme Environments Program under the direction of Dr. Ali Sayir. We would like to thank Dr. Kateryna Artyushkova of University of New Mexico for the excellent XPS experimental measurements, spectral analysis, and discussion. We would also like to thank David Wilt and David Bowers of AFRL for use of DHR instruments.

## 7. REFERENCES

[1] D. Hastings and H. Garrett, *Spacecraft-environment interactions*: Cambridge university press, 2004.

[2] T. Paulmier, R. Hanna, M. Belhaj, B. Dirassen, D. Payan, N. Balcon, *et al.*, "Aging effect and induced electric phenomena on dielectric materials irradiated with high energy electrons," *Plasma Science, IEEE Transactions on*, vol. 41, pp. 3422-3428, 2013.

[3] L. Levy, T. Paulmier, B. Dirassen, C. Inguimbert, and M. Van Eesbeek, "Aging and Prompt Effects on Space Material Properties," *Plasma Science, IEEE Transactions on*, vol. 36, pp. 2228-2237, 2008.

[4] L. Kan and K. C. Kao, "Photoconduction in polyimide," in *Electrical Insulation, 1990., Conference Record of the 1990 IEEE International Symposium on*, 1990, pp. 84-87.

[5] J. Davenas, X. Xu, G. Boiteux, and D. Sage, "Relation between structure and electronic properties of ion irradiated polymers," *Nuclear Instruments and Methods in Physics Research Section B: Beam Interactions with Materials and Atoms*, vol. 39, pp. 754-763, 1989.

[6] T. Hioki, S. Noda, M. Sugiura, M. Kakeno, K. Yamada, and J. Kawamoto, "Electrical and optical properties of ion-irradiated organic polymer Kapton H," *Applied Physics Letters*, vol. 43, pp. 30-32, 1983.

[7] J. Salvetat, J. Costantini, F. Brisard, and L. Zuppiroli, "Onset and growth of conduction in polyimide kapton induced by swift heavy-ion irradiation," *Physical Review B*, vol. 55, p. 6238, 1997.

[8] C. P. Ennis and R. I. Kaiser, "Mechanistical studies on the electron-induced degradation of polymethylmethacrylate and Kapton," *Physical Chemistry Chemical Physics*, vol. 12, pp. 14902-14915, 2010.

[9] A. Sim, "Unified model of charge transport in insulating polymeric materials," 2013.

[10] J. Brunson, "Hopping conductivity and charge transport in low density polyethylene," Ph.D., Physics, Utah State University, 2010.

[11] H. J. Wintle, "Surface-Charge Decay in Insulators with Nonconstant Mobility and with Deep Trapping," *Journal of Applied Physics*, vol. 43, pp. 2927-2930, 1972.

[12] R. Hoffmann, D. Ferguson, A. Wheelock, and J. Patton, "The Spacecraft Charging and Instrument Calibration Laboratory: A New Frontier in American Spacecraft Charging R&D," in *50th AIAA Aerospace Sciences Meeting including the New Horizons Forum and Aerospace Exposition*, p. 716.

[13] R. Cooper and R. Hoffmann, "JUMBO SPACE ENVIRONMENT SIMULATION AND SPACECRAFT CHARGING CHAMBER CHARACTERIZATION," *Air Force Technical Report*, 2015.

[14] A. Glassford and C. Liu, "Outgassing rate of multilayer insulation materials at ambient temperature," *Journal of Vacuum Science & Technology*, vol. 17, pp. 696-704, 1980.

[15] M. Berger, "ESTAR, PSTAR, and ASTAR: Computer programs for calculating stopping-power and range tables for electrons, protons, and helium ions," *Unknown*, vol. 1, 1992.

[16] Sheldahl. (2015, July 14). *The Red Book*. Available: http://www.sheldahl.com/Products/WebPages/RedBook.aspx

[17] D. N. Baker, "Effects of hostile space weather on satellite operations," in *Electromagnetic Compatibility (EMC), 2011 IEEE International Symposium on*, 2011, pp. 306-311.

[18] G. Ginet, T. O'Brien, S. Huston, W. Johnston, T. Guild, R. Friedel, *et al.*, "AE9, AP9 and SPM: New models for specifying the trapped energetic particle and space plasma environment," *Space science reviews*, vol. 179, pp. 579-615, 2013.

[19] R. Toomer and T. Lewis, "Charge trapping in corona-charge polyethylene films," *Journal of Physics D: Applied Physics*, vol. 13, p. 1343, 1980.

[20] R. Li, C. Li, S. He, M. Di, and D. Yang, "Damage effect of keV proton irradiation on aluminized Kapton film," *Radiation Physics and Chemistry*, vol. 77, pp. 482-489, 2008.

[21] T. Steckenreiter, E. Balanzat, H. Fuess, and C. Trautmann, "Pyrolytic effects induced by energetic ions in polymers," *Nuclear Instruments and Methods in Physics Research Section B: Beam Interactions with Materials and Atoms*, vol. 151, pp. 161-168, 5/2/ 1999.

[22] T. Venkatesan, "High energy ion beam modification of polymer films," *Nuclear Instruments and Methods in Physics Research Section B: Beam Interactions with Materials and Atoms*, vol. 7–8, Part 2, pp. 461-467, 3// 1985.

[23] D. J. T. Hill and J. L. Hopewell, "Effects of 3 MeV proton irradiation on the mechanical properties of polyimide films," *Radiation Physics and Chemistry*, vol. 48, pp. 533-537, 11// 1996.

[24] J.-P. Salvetat, A. Berthault, F. Brisard, J. Costantini, and J. Davenas, "ESR study of the insulator-conductor transition in polyimide kapton induced by swift heavy ion irradiations," *Radiation effects and defects in solids*, vol. 136, pp. 267-272, 1995.

[25] G. Marletta, "Chemical reactions and physical property modifications induced by keV ion beams in polymers," *Nuclear Instruments and Methods in Physics Research Section B: Beam Interactions with Materials and Atoms*, vol. 46, pp. 295-305, 2/1/ 1990.